Influence of Hydrophobic Mismatching on Membrane Protein Diffusion

Gernot Guigas and Matthias Weiss

Cellular Biophysics Group (BIOMS), German Cancer Research Center, Heidelberg, Germany

ABSTRACT   The observation of membrane domains in vivo and in vitro has triggered a renewed interest in the size-dependent diffusion of membrane inclusions (e.g., clusters of transmembrane proteins and lipid rafts). Here, we have used coarse-grained membrane simulations to quantify the influence of a hydrophobic mismatch between the inclusion's transmembrane portion and the surrounding lipid bilayer on the diffusive mobility of the inclusion. Our data indicate only slight changes in the mobility ($<30\%$) when altering the hydrophobic mismatch, and the scaling of the diffusion coefficient D is most consistent with previous hydrodynamic predictions, i.e., with the Saffman-Delbruck relation and the edgewise motion of a thin disk in the limit of small and large radii, respectively.

The long prevailing view on biomembranes as a fluid mosaic (1) has undergone a major change since a variety of membrane domains, e.g., clusters of lipids and/or proteins, have been postulated and, in part, shown to exist in living cells and artificial bilayers (see, e.g., (2–4) for reviews). The observation of larger entities on membranes has triggered an increased interest in the size-dependent mobility of membrane inclusions. Based on the seminal work by Saffman and Delbruck (5) and its subsequent extension (6), very recently an approximate analytical expression for the mobility μ_m of an incompressible, cylindrical inclusion of radius R in a membrane has been derived (7):

$$\mu_m = \frac{(2\xi - 1)\ln(\xi) - \gamma + 8\xi/\pi}{4\pi\eta_m h\left(1 + 8\xi^3\ln(\xi)/\pi + \dfrac{a_1\xi^{b_1}}{1 + a_2\xi^{b_2}}\right)}. \tag{1}$$

Here, $\xi = R\eta_c/(h\eta_m)$ with h being the bilayer thickness and η_m, η_c denoting the viscosities of the membrane and the adjacent fluid, respectively; $\gamma \approx 0.5772$ is Euler's constant, $b_1 = 2.74819$, $b_2 = 0.614465$, and $a_1 = 0.433274$, $a_2 = 0.670045$. The diffusion coefficient is determined by $D = \mu_m k_B T$.

For small radii ($\xi \to 0$), Eq. 1 converges toward the familiar result $D \sim \ln(1/\xi) - \gamma$ (5), while for $\xi \to \infty$ the result for an edgewise motion of a thin disk, $D \sim 1/\xi$, is recovered (6). Indeed, both regimes have been supported by a number of experiments (7–10) and simulations (11).

Owing to the assumptions in the mean-field approach (lateral motion of a cylinder in a two-dimensional fluid; see (5,6)), Eq. 1 does not include any information on how the mobility μ_m changes when the inclusion locally perturbs the lipid bilayer, e.g., due to a hydrophobic mismatch between the inclusion's transmembrane portion and the hydrophobic core of the bilayer (see (12) for a recent review on hydrophobic mismatching).

Recently, a correction to the results of the literature (5,6), which included local bilayer perturbations by a coupling constant c, has been derived to explain experimental observations on a scaling $D \sim 1/R$ even for $\xi \ll 1$ (13,14):

$$\mu = \mu_m/(1 + c\xi\mu_m). \tag{2}$$

Yet, as the derivation of Eq. 2 relied on a few ad hoc assumptions, it remained somewhat unclear if it indeed reconciles the conflicting experimental results and if it is capable of properly describing the diffusion of membrane inclusions with a hydrophobic mismatch.

To thoroughly probe the modulation of the mobility of membrane inclusions via hydrophobic mismatching, we have employed coarse-grained membrane simulations (dissipative particle dynamics; see, e.g., (15) for an introduction). Between any two beads i, j with a distance $r_{ij} = |\mathbf{r}_{ij}| = |\mathbf{r}_i - \mathbf{r}_j| \leq r_0$, a linear repulsive force $\mathbf{F}_{ij}^C = a_{ij}(1 - r_{ij}/r_0)\hat{\mathbf{r}}_{ij}$ was imposed (with $\hat{\mathbf{r}}_{ij} = \mathbf{r}_{ij}/r_{ij}$). The hydrophobicity of beads was tuned via the interaction energies a_{ij} while bonds within lipids and proteins were modeled via a harmonic potential $U(\mathbf{r}_i, \mathbf{r}_{i+1}) = k(r_{i,i+1} - l_0)^2/2$ between the respective beads. Lipids and proteins were given an additional bending stiffness via the potential $V(\mathbf{r}_{i-1}, \mathbf{r}_i, \mathbf{r}_{i+1}) = \kappa[1 - \cos(\phi)]$ with $\cos\phi = \hat{\mathbf{r}}_{i-1,i} \cdot \hat{\mathbf{r}}_{i,i+1}$. For the thermostat, dissipative and random forces were given by $\mathbf{F}_{ij}^D = -\gamma_{ij}(1 - r_{ij}/r_0)^2(\hat{\mathbf{r}}_{ij} \cdot \mathbf{v}_{ij})\hat{\mathbf{r}}_{ij}$ and $\mathbf{F}_{ij}^R = \sigma_{ij}(1 - r_{ij}/r_0)\zeta_{ij}\hat{\mathbf{r}}_{ij}$, respectively, when $r_{ij} \leq r_0$. Here, $\mathbf{v}_{ij} = \mathbf{v}_i - \mathbf{v}_j$ while ζ_{ij} is an independent random variable with zero mean; γ_{ij} and σ_{ij} are related via the fluctuation-dissipation theorem $\sigma_{ij}^2 = 2\gamma_{ij}k_B T$ (16).

We have set the interaction cutoff r_0, the bead mass m, and the thermostat temperature $k_B T$ to unity while $\gamma_{ij} = 9/2$, $k = $

$100 \, k_{\mathrm{B}}T/r_0^2$, $l_0 = 0.45r_0$, $\kappa = 20 \, k_{\mathrm{B}}T$, $a_{\mathrm{HT}} = a_{\mathrm{WT}} = 100 \, k_{\mathrm{B}}T$, and $a_{\mathrm{WW}} = a_{\mathrm{HH}} = a_{\mathrm{TT}} = a_{\mathrm{WH}} = 25 \, k_{\mathrm{B}}T$ (indices W,H,T denoting water, lipid head, and lipid tail bead, respectively).

Lipids were modeled as linear chains (HT_3), while proteins were modeled as solid hexagons of HT_nH chains with a diameter of $2K + 1$ chains (see also (11) for details). By changing the number of hydrophobic beads, n, in the protein, the hydrophobic mismatch could be tuned. Water surrounding the lipid bilayer was modeled by individual beads (see above for repulsion parameters), thereby allowing for the simulation of a fully hydrated membrane. The equations of motion were integrated with a velocity Verlet scheme (10^6 time steps with $\Delta t = 0.01$) using periodic boundary conditions (membrane patch size $40r_0 \times 40r_0$). Conversion to SI units may be done ($r_0 \equiv 1 \, \mathrm{nm}$, $\Delta t \equiv 90 \, \mathrm{ps}$) by gauging the membrane thickness and the lipids' diffusion coefficient (11).

We first checked how inclusions with n hydrophobic transmembrane layers locally deform the lipid bilayer. In agreement with previous predictions (17), we observed an exponential profile for the membrane thickness of

$$h(r) = h_0 + \Delta_{\mathrm{h}} e^{-\mathrm{r}/\lambda}, \qquad (3)$$

with $h_0 \approx 3.5r_0$ and $\Delta_{\mathrm{h}} \sim n$ (Fig. 1). Notably, the perturbation length λ did not vary much with the inclusion's radius R but stayed rather constant ($\lambda \approx r_0$). While $n = 3$ showed a strong negative hydrophobic mismatch, $n = 5, 6$ showed an increasing positive mismatch, whereas at $n = 4$ the mismatch vanished.

We next monitored the inclusions' diffusion for various radii and hydrophobic mismatches. In particular, we deter-
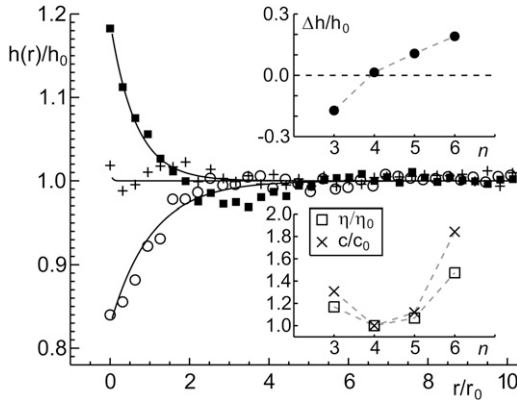
mined the diffusion coefficients by fitting the arithmetically averaged mean-square displacement (based on five independent runs). The resulting data D/D_{L} (D_{L} being the diffusion coefficient of a single lipid) were fitted with Eq. 1 and Eq. 2. In particular, we used a global fit approach for both functions: For Eq. 2, we demanded that the fit parameters $R_{\mathrm{c}} = h\eta_{\mathrm{m}}/\eta_{\mathrm{c}}$ and η_{m} stay constant for all data sets ($n = 3, 4, 5, 6$), while c was allowed to vary with n. The rationale behind this choice was that all perturbation information is reduced to the coupling parameter c (see (14)). In contrast, for Eq. 1 we only required the ratio $R_{\mathrm{c}}/\eta_{\mathrm{m}}$ to stay constant, while η_{m} could vary with n. The rationale behind that was that lipids near to the inclusion are more or less confined in their configuration (depending on the hydrophobic mismatch), thus yielding a (slightly) varying effective membrane viscosity.

Both Eq. 1 and Eq. 2, fitted the numerical data almost equally well (as judged via the root-mean-square percent deviation; see also Fig. 2). As anticipated, the effective viscosity η_{m} in Eq. 1 and the coupling constant c in Eq. 2 showed a systematic variation with the hydrophobic mismatch, i.e., both quantities were smallest for $n = 4$ and increased for $n = 3, 5, 6$ (Fig. 1, inset). Thus, at this level one cannot claim one of the fitting functions to perform better than the other, albeit one might have expected that c shows a more drastic decrease for a vanishing hydrophobic mismatch ($n = 4$). In fact, another criterion provided more solid evidence that Eq. 1 is the better approach to describe the mobility changes induced by hydrophobic mismatching. The critical radius R_{c} beyond which the inclusion's contact with the adjacent solvent dominates the friction (6) is very different for the two fits. While $R_{\mathrm{c}} \approx 7.1r_0$ for Eq. 1 is much larger than the size of a single lipid, Eq. 2 yields $R_{\mathrm{c}} \approx 1.6r_0$ which appears somewhat small. If $R_{\mathrm{c}} = h\eta_{\mathrm{m}}/\eta_{\mathrm{c}}$ was approximately unity, as predicted by Eq. 2, the membrane viscosity η_{m} would have to be smaller than the solvent viscosity η_{c} since $h \approx 3.5r_0$. This, however, is

FIGURE 1 The bilayer thickness $h(r)$ (symbols) in a distance r from the inclusion deviates exponentially from the unperturbed thickness h_0 for negative ($n = 3$, open circles), vanishing ($n = 4$, crosses), and positive ($n = 6$, solid squares) hydrophobic mismatch. Solid lines are fits according to Eq. 3. (Upper inset) The relative variation of the thickness, defining the strength of the hydrophobic mismatch, varies systematically with n and almost vanishes for $n = 4$. (Lower inset) The relative change of the effective membrane viscosity η_{m} (Eq. 1) and of the coupling constant c (Eq. 2) both vary with the hydrophobic mismatch (indicated here via the parameter n). Values η_0 and c_0 denote the values obtained for a vanishing hydrophobic mismatch ($n = 4$).
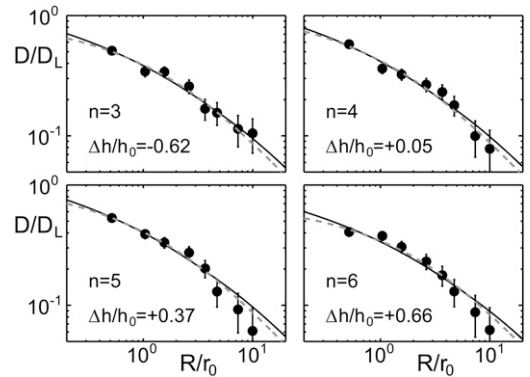

FIGURE 2 The size-dependent diffusion coefficient D of transmembrane inclusions with varying hydrophobic mismatch (symbols) is equally well fitted by Eq. 1 (solid) and Eq. 2 (dashed). Please note that D is normalized by the diffusion coefficient D_{L} of a single lipid. Since the fitting parameter $R_{\mathrm{c}} = h\eta_{\mathrm{m}}/\eta_{\mathrm{c}}$ takes on too-small values when using Eq. 2 (see also main text), Eq. 1 appears to be the more appropriate fit function.

in contradiction to observations in experiments (see, e.g., (7,10)). Therefore, we argue that Eq. 1 better captures the mobility of membrane inclusions that have a hydrophobic mismatch with their surrounding lipid bilayer. The hydrophobic mismatch thus leads to a change in the effective membrane viscosity but does not alter the gross scaling behavior of the diffusive mobility. Indeed, introducing a hydrophobic mismatch only slightly alters the inclusion's mobility (some 30%; see Fig. 1, *inset*). Still, in a biological problem this altered diffusion may play an important role, e.g., in the context of protein sorting (18).

Translating our above results to SI units, one obtains a typical membrane viscosity ≈ 0.09 Pas that is 10–20% lower than experimentally found values (8). The viscosity of the surrounding solvent, $\eta_c \approx 0.04$ Pas (extracted from an independent simulation of a globular object's three-dimensional diffusion in pure solvent), at first glance appears somewhat high. While one could, in principle, aim at approaching the ideal situation of a pure lipid bilayer in water ($\eta_c \approx 0.001$ Pas) by altering the DPD parameters, the strongly viscoelastic nature of intracellular fluids like the cytoplasm (19) suggests that assuming a fairly high solvent viscosity η_c may not be so errant in the biological context. Thus, a low value of R_c, as depicted above, may indeed be relevant in vivo. As a consequence, a strong size dependence $D \sim 1/R$ of the diffusion of protein clusters and rafts can occur already for moderate radii, e.g., beyond some 10 nm.

In conclusion, we have tested how hydrophobic mismatching alters the diffusional mobility of membrane inclusions, e.g., transmembrane proteins. Our data on the size-dependent mobility are most consistent with the results derived in the literature (5–7) when assuming that hydrophobic mismatching slightly alters the effective membrane viscosity due to local constraints for the lipids' configuration in the vicinity of the inclusion. Corrections to Eq. 1 as derived in Naji et al. (14) also fit our data well, yet the interpretation of the fitting parameters appears problematic. This, however, may be different under the experimental conditions explored in Gambin et al. (13) where Eq. 2 might be more applicable.

ACKNOWLEDGMENTS

REFERENCES and FOOTNOTES

1. Singer, S. J., and G. L. Nicholson. 1972. The fluid mosaic model of the structure of cell membranes. *Science*. 175:720–731.

2. Simons, K., and E. Ikonen. 1997. Functional rafts in cell membranes. *Nature*. 119:569–572.

3. Edidin, M. 2003. The state of lipid rafts: from model membranes to cells. *Annu. Rev. Biophys. Biomol. Struct.* 32:257–283.

4. Veatch, S. L., and S. L. Keller. 2005. Seeing spots: complex phase behavior in simple membranes. *Biochim. Biophys. Acta*. 1746:172–185.

5. Saffman, P. G., and M. Delbrück. 1975. Brownian motion in biological membranes. *Proc. Natl. Acad. Sci. USA*. 72:3111–3113.

6. Hughes, B. D., B. A. Pailthorpe, and L. R. White. 1981. The translational and rotational drag on a cylinder moving in a membrane. *J. Fluid Mech.* 110:349–372.

7. Petrov, E. P., and P. Schwille. 2008. Translational diffusion in lipid membranes beyond the Saffman-Delbruck approximation. *Biophys. J.* 94:L41–L43.

8. Peters, R., and R. J. Cherry. 1982. Lateral and rotational diffusion of bacteriorhodopsin in lipid bilayers: Experimental test of the Saffman-Delbruck equations. *Proc. Natl. Acad. Sci. USA*. 79:4317–4321.

9. Lee, C. C., and N. O. Petersen. 2003. The lateral diffusion of selectively aggregated peptides in giant unilamellar vesicles. *Biophys. J.* 84:1756–1764.

10. Cicuta, P., S. L. Keller, and S. L. Veatch. 2007. Diffusion of liquid domains in lipid bilayer membranes. *J. Phys. Chem. B*. 111:3328–3331.

11. Guigas, G., and M. Weiss. 2006. Size-dependent diffusion of membrane inclusions. *Biophys. J.* 91:2393–2398.

12. Jensen, M., and O. G. Mouritsen. 2004. Lipids do influence protein function—the hydrophobic matching hypothesis revisited. *Biochim. Biophys. Acta*. 1666:205–226.

13. Gambin, Y., R. Lopez-Esparza, M. Reffay, E. Sierecki, N. Gov, M. Genest, R. Hodges, and W. Urbach. 2006. Lateral mobility of proteins in liquid membranes revisited. *Proc. Natl. Acad. Sci. USA*. 103:2098–2102.

14. Naji, A., A. J. Levine, and P. A. Pincus. 2007. Corrections to the Saffman-Delbruck mobility for membrane-bound proteins. *Biophys. J.* 93:L49–L51.

15. Nikunen, P., M. Karttunen, and I. Vattulainen. 2003. How would you integrate the equations of motion in dissipative particle dynamics simulations? *Comput. Phys. Commun.* 153:407–423.

16. Español, P., and P. Warren. 1995. Statistical mechanics of dissipative particle dynamics. *Europhys. Lett.* 30:191–196.

17. Fattal, D. R., and A. Ben-Shaul. 1993. A molecular model for lipid-protein interaction in membranes: the role of hydrophobic mismatch. *Biophys. J.* 65:1795–1809.

18. Ronchi, P., S. Colombo, M. Francolini, and N. Borgese. 2008. Transmembrane domain-dependent partitioning of membrane proteins within the endoplasmic reticulum. *J. Cell Biol.* 181:105–118.

19. Guigas, G., C. Kalla, and M. Weiss. 2007. Probing the nanoscale viscoelasticity of intracellular fluids in living cells. *Biophys. J.* 93:316–323.